Dynamical properties of semidilute solutions of hydrogen-bonded supramolecular polymers

Eric Buhler,[1] Sauveur-Jean Candau,[2] Elena Kolomiets,[2] and Jean-Marie Lehn[2]
[1]*Matière et Systèmes Complexes, UMR CNRS 7057, Université Paris 7-Denis Diderot, Bâtiment Condorcet, CC 7056, 75205 Paris cedex 13, France*
[2]*Laboratoire de Chimie Supramoléculaire, ISIS, UMR CNRS 7006, Université Louis Pasteur, 8 Allée Gaspard Monge, 67000 Strasbourg, France*
(Received 6 September 2007; published 21 December 2007)

The dynamical properties of semidilute solutions of supramolecular polymers formed from molecular recognition directed association between monomers bearing complementary hydrogen bonding groups were investigated by rheological and dynamic light scattering experiments. The steady-state flow curves showed a shear banding type instability, namely the occurrence of a stress plateau σ_p above a critical shear rate $\dot{\gamma}_c$. The values of σ_p and $\dot{\gamma}_c$ were found to be of the same order of magnitude as those of the elastic plateau modulus and the inverse stress relaxation time, respectively. The above features are in agreement with the theoretical predictions based on the reptation model. Dynamic light scattering experiments showed the presence in the autocorrelation function of the concentration fluctuations of a slow viscoelastic relaxation process that is likely to be of Rouse type.

DOI: 10.1103/PhysRevE.76.061804 PACS number(s): 83.80.Rs, 82.70.−y, 83.80.Kn, 83.80.Qr

I. INTRODUCTION

Reversible supramolecular polymers [1–42] can be formed from the association of two homoditopic heterocomplementary monomers through sextuple hydrogen-bonding arrays [17,38,39]. Recent small-angle neutron scattering (SANS) studies showed that such monomers in decane solutions self-assemble into long semiflexible fibrils with persistence length of ~18 nm and contour length increasing upon increasing monomer concentration and/or decreasing temperature [38,39]. The cross-section and the linear density of the fibrils were found to be constant over large concentration and temperature ranges and equal to (10.8 ± 0.5) nm^2 and (5200 ± 500) g mol^{-1} nm^{-1}, respectively. This suggest that the fibrils are formed from few macromolecular chains likely aggregated via a stacking of the aromating rings contained in the monomers [38,39]. In the dilute regime the fibrils are linear but in the vicinity of the critical rod overlap concentration C^*, the SANS data suggest the formation of highly branched entities. Beyond C^*, the systems look like gels.

The aim of this study is to investigate the dynamical properties of such supramolecular polymers in the semidilute regime. We have first addressed the issue of whether the concentrated systems were crosslinked physical gels or highly viscous solutions. For this purpose, we have performed linear and nonlinear viscoelasticity experiments. The results obtained by the latter technique in the semidilute regime clearly indicate that the systems behave as extremely viscous solutions showing a mechanical instability of shear banding type, similar to that observed in wormlike micellar solutions [43,44]. Beyond $\sim 5C^*$ the systems do not flow at times scale of days. Estimates of the longest time of the stress relaxation and of the plateau modulus were obtained by combining linear and nonlinear viscoelastic experiments and compared to the inverse critical shear rate and the stress plateau respectively associated with the shear instability.

To obtain more insight in the local concentration fluctuations we also performed dynamic light scattering (DLS) experiments both in the dilute and semidilute regimes.

II. MATERIALS AND METHODS

A. Samples characteristics

The strong affinity of the DAD-DAD (D=donor, A=acceptor) hydrogen-bonding sites for double-faced cyanuric acid type ADA-ADA wedges drives the supramolecular polymeric assembly in organic solvents of low polarity as shown in Fig. 1 where the bisreceptor AA9 bearing decanoyl side chains is associated with the biswedge BB.

The synthesis of the homoditopic receptor AA9 and the ditopic substrate BB whose formula are given in Fig. 1 has been described in a previous publication [17,38].

Bisreceptor AA9 and biswedge BB are almost insoluble in decane as individual compounds. In contrast, their mixtures in 1:1 stoichiometry dissolve readily in decane under heating

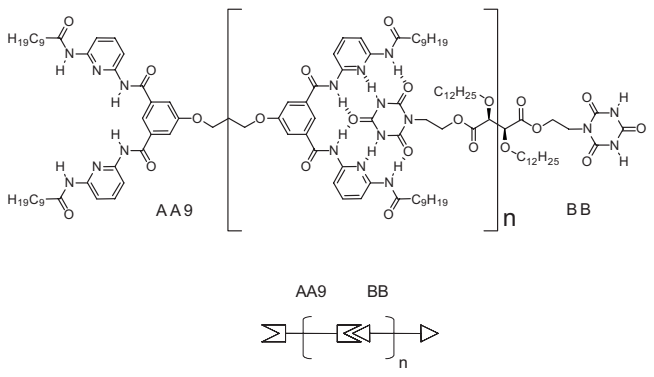

FIG. 1. Linear supramolecular polymer $[AA9:BB]_n$ formed by H-bond mediated molecular recognition between heterocomplementary binding sites of homoditopic bisreceptor AA9 and homoditopic biswedge BB.

to form transparent solutions in decane, that are stable over time and thermal cycles. A sharp increase of viscosity is observed at the crossover concentration C^* between dilute and semidilute regimes, that is the concentration beyond which the polymeric aggregates start to overlap each other. The crossover concentration C^* was determined from viscosimetric measurements and found to be ~ 2.2 mM at $T=25$ °C.

B. Rheological techniques

Oscillatory studies were performed with a HAAKE RS rheometer, using a cone-plate geometry (diameter 60 mm, 1°). As this apparatus can be used in both controlled stress (CS) and controlled strain (CD) modes, the experiments were carried out employing both of these modes in the linear regime. The latter condition was verified by measuring the storage and loss moduli as a function of the shear stress at frequencies 1 Hz and 0.1 Hz.

The viscometry measurements on low viscosity solutions of $[\mathrm{AA9:BB}]_n$ in decane were performed on a Contraves LS 30 low-shear rheometer equipped with a Couette 2T-2T measuring system.

Nonlinear rheological experiments on highly viscous polymer solutions of $[\mathrm{AA9:BB}]_n$ in decane were performed with a HAAKE RS 100 rheometer in a controlled stress (CS) mode, equipped with a cone-plate geometry (diameter 60 mm, 1°).

C. Dynamic light scattering

In the dynamic light scattering experiments (DLS), the normalized time autocorrelation function, $g^{(2)}(q,t)$, is measured as a function of the scattered wave vector, q, given by $q=(4\pi n/\lambda)\sin(\theta/2)$, where n is the refractive index of the solvent (1.409 for decane at 20 °C), and θ is the scattering angle. In our experiments, θ was varied between 30° and 130°, which corresponds to scattering wave vectors, q, in the range from 8×10^{-3} to 2.9×10^{-2} nm^{-1}. The measurements used a standard setup of a spectrometer equipped with a laser (Melles Griot, 58-GCA-series green diode-pumped solid-state laser) operating at $\lambda=532$ nm, an ALV-5000 correlator (ALV, Langen-Germany Instruments), a variable-angle detection system, and a temperature-controlled sample cell (ALV). The scattering spectrum was measured using a fiber optical detector and an avalanche photodiode (Perkin Elmer, model SPCM-AQR-13-FC) and a 100 μm pinhole.

The experimental signal is the normalized time autocorrelation function of the scattered intensity [45]:

$$g^{(2)}(q,t)=\frac{\langle I(q,0)I(q,t)\rangle}{\langle I(q,0)\rangle^2}. \tag{1}$$

The latter can be expressed in terms of the field autocorrelation function or equivalently in terms of the autocorrelation function of the concentration fluctuations, $g^{(1)}(q,t)$, through

$$g^{(2)}(q,t)-1=\alpha+\beta|g^{(1)}(q,t)|^2, \tag{2}$$

where α is the baseline (varying between 2×10^{-5} and 2×10^{-4} depending on the scattering angle and/or the concentration) and β the coherence factor, which in our experiments is equal to 0.7–0.9. The normalized dynamical correlation function, $g^{(1)}(q,t)$, of polymer concentration fluctuations is defined as

$$g^{(1)}(q,t)=\frac{\langle \delta c(q,0)\delta c(q,t)\rangle}{\langle \delta c(q,0)^2\rangle}, \tag{3}$$

where $\delta c(q,t)$ and $\delta c(q,0)$ represent fluctuations of the polymer concentration at time t and zero, respectively.

In our experiments, the dilute solutions were characterized by a single relaxation mechanism with a characteristic relaxation time inversely proportional to q^2. For these solutions we have adopted the classical cumulant analysis [46]. The extrapolation of $(\tau_c q^2)^{-1}$ to $q=0$, where τ_c is the average relaxation time of $g^{(1)}(q,t)$, yields the mutual diffusion coefficient D. The latter is related to the average apparent hydrodynamic radius, R_H, of the supramolecular assemblies through

$$D=\frac{kT}{6\pi\eta_s R_H}, \tag{4}$$

where k is the Boltzmann constant, η_s the solvent viscosity, and T the absolute temperature.

For semidilute solutions characterized by several relaxation mechanisms we used the Contin method based on the inverse Laplace transform of $g^{(1)}(q,t)$ [47]. If the spectral profile of the scattered light can be described by a multi-Lorentzian curve, then $g^{(1)}(q,t)$ can be written as

$$g^{(1)}(q,t)=\int_0^\infty G(\Gamma)\exp(-\Gamma t)d\Gamma, \tag{5}$$

where $G(\Gamma)$ is the normalized decay constant distribution.

III. EXPERIMENTAL RESULTS

Rheological experiments were performed on systems with two concentrations: 3.5 mM $(C/C^*\sim1.5)$ and 5 mM $(C/C^*\sim2.2)$. DLS experiments were carried out in a concentration range spanning both the dilute and semidilute regimes $(0.5\leqslant C/C^*\leqslant5)$. All the experiments were conducted at $T=25$ °C.

A. Oscillatory experiments

Figure 2(a) shows the frequency dependencies of the storage modulus $G'(\omega)$ and of the loss modulus $G''(\omega)$ obtained with both CS and CD modes. The two different shearing modes give concordant results, with G' larger than G'', both being only slightly frequency dependent. This behavior is a gel-like response similar to those previously reported for weak, physically cross-linked gels [48] or associating polymers [49]. Still, one cannot exclude that $G'(\omega)$ and $G''(\omega)$ cross over each other at a frequency lower than the experimentally accessible frequency range, that is 0.05 rad/s. As a matter of fact, the flow experiments reported in the following show that the samples behave like viscoelastic fluids with very long stress relaxation time rather than gels exhibiting a

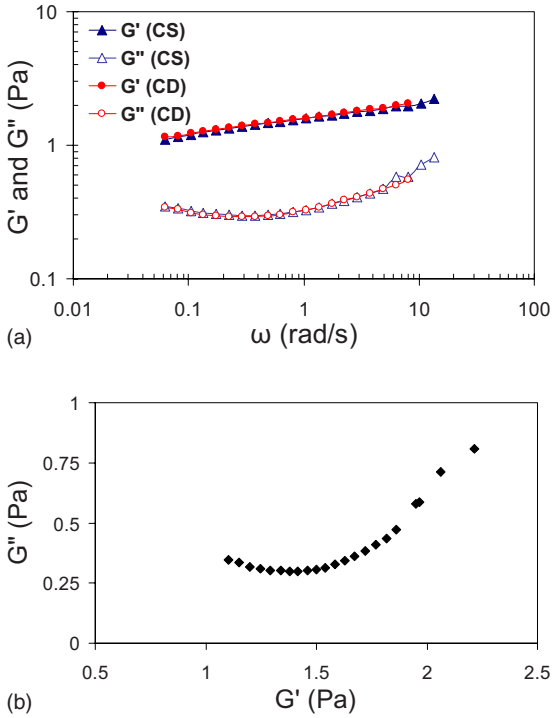

FIG. 2. (Color online) Viscoelastic spectra for a 5 mM $[AA9:BB]_n$ solution in decane: (a) Real and imaginary parts of the shear modulus versus angular frequency; (b) Cole-Cole plot at 25 °C.

yield stress. It must also be mentioned that $G'(\omega)$ does not exhibit a real plateau but slightly increases with frequency. This is generally observed for both regular and equilibrium polymer systems [29]. Generally, the plateau modulus G_0 is determined from the value of the crossover between $G'(\omega)$ and $G''(\omega)$. In the present study the crossover value is inaccessible but from the pseudo plateau of Fig. 2(a) one can estimate that G_0 is 1.7±0.3 Pa. The Cole-Cole representation G'' versus G' shown in Fig. 2(b) exhibits an upturn at high frequency indicating a faster relaxation process with a characteristic relaxation time shorter than 20 ms.

B. Flow experiments

Figure 3 shows the variation of the viscosity versus the shear stress σ obtained for the low viscosity solution at the concentration $C=3.5$ mM, close to C^* $(C/C^* \sim 1.5)$. The flow behavior of the 3.5 mM solution is typical of a classical polymer, characterized by a Newtonian plateau at low shear stresses corresponding to the regime $\dot{\gamma}T_R < 1$, where $\dot{\gamma}$ is the shear rate and T_R the stress relaxation time, followed by a smooth viscosity decrease in the shear thinning zone.

The relaxation time can be measured from a startup experiment in the linear regime $(\dot{\gamma}T_R < 1)$ such as that illustrated by Fig. 4 that shows the transient response of the viscosity $\eta = \sigma/\dot{\gamma}$ (σ, shear stress) to a shear rate $\dot{\gamma}=0.1$ s^{-1} for a solution at $C=3.5$ mM. One observes the typical linear response of a Maxwellian fluid that is a linear increase of the viscosity at times shorter than the Maxwell relaxation time

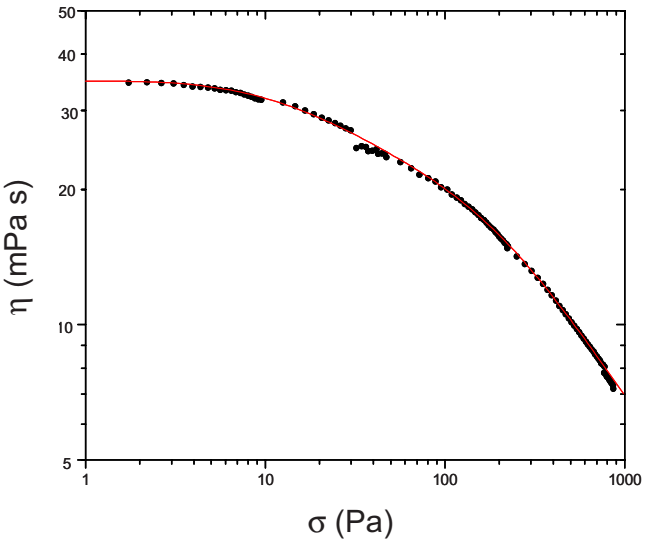

FIG. 3. (Color online) Viscosity as a function of the shear stress for a solution of $[AA9:BB]_n$ in decane at $C=3.5$ mM and $T=25$ °C. The continuous line is a guide for the eyes.

T_R and then a saturation for $t \gg T_R$ at the constant value of ~34 mPa s.

In the linear regime, the transient behavior is described by the following equation:

$$\eta(t) = \eta_0[1 - \exp(-t/T_R)]. \quad (6)$$

The fit of the data of Fig. 4 by the above equation leads to $T_R=3.6$ s and $\eta_0=34.25$ mPa s. The value of the shear modulus G_0 is obtained from the relation

$$\eta_0 = G_0 T_R. \quad (7)$$

One obtains $G_0=9.5$ mPa that is a very low value, which is not surprising taking into account that the concentration of the solution is hardly above C^*.

The flow behavior of the semi-dilute solution at $C=5$ mM is quite different as shown in Fig. 5. At low shear stress one observes a plateau followed by an abrupt decrease of the viscosity at a critical shear stress σ_p then by a second

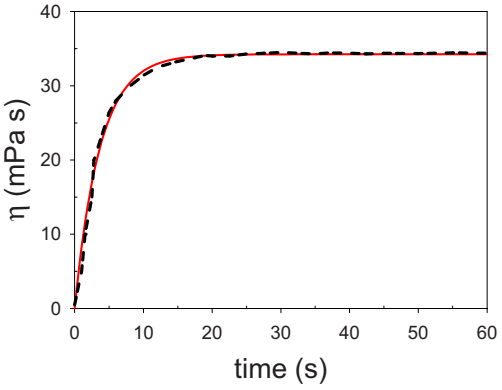

FIG. 4. (Color online) Variation of the viscosity with time for a $[AA9:BB]_n$ solution at $C=3.5$ mM at $\dot{\gamma}=0.1$ s^{-1} and 25 °C. The continuous line represents the fit of the data.

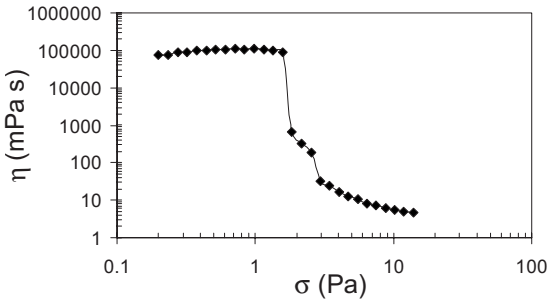

FIG. 5. Viscosity as a function of the shear stress for a 5 mM $[AA9:BB]_n$ solution in decane at $T=25\,^{\circ}C$.

smaller drop at high shear stress. The flow curve represented in Fig. 5 was measured with the CS mode by increasing the shear stress by rectangular steps and waiting at each step for 15 min.

To obtain an accurate value of σ_p sweep shear stress experiments were carried out in a narrow range of stresses close to σ_p. Figure 6 shows the transient responses to variable shear stresses applied for periods of 5 min. The drop of viscosity occurs for $\sigma_p \sim 1.39$ Pa.

We have also verified the reversibility under stress of the system. Figure 7 illustrates the recovery of the 5 mM solution after being submitted to a stress $\sigma \gg \sigma_p$. First, the solution was sheared at $\sigma=5$ Pa for 5 min, so that the viscosity of the solution becomes very low. Upon applying immediately after a shear stress of 1 Pa, the initial viscosity of the solution was recovered in a time of the order of magnitude of the Maxwell time given by Eq. (7) using $\eta_0=170$ Pa s and $G_0=1.7$ Pa ($T_R \sim 100$ s).

C. Dynamic light scattering

DLS experiments provide evidence of the structural evolution of the system as the concentration is increased. In the dilute regime up to slightly above C^* ($1.2\ \text{mM} \leqslant C \leqslant 3.5$ mM) the autocorrelation function of the scattered field $g^{(1)}(q,t)$ is close to a single exponential.

The average characteristic relaxation time τ_c varies as q^{-2}. The mutual diffusion coefficient D, given by $(\tau_c q^2)^{-1}$, yields the hydrodynamic radius through Eq. (4).

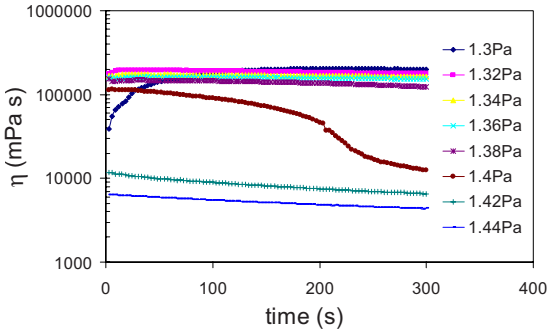

FIG. 6. (Color online) Viscosity as a function of time at different shear stresses for the 5 mM solution of $[AA9:BB]_n$ in decane at 25 °C.

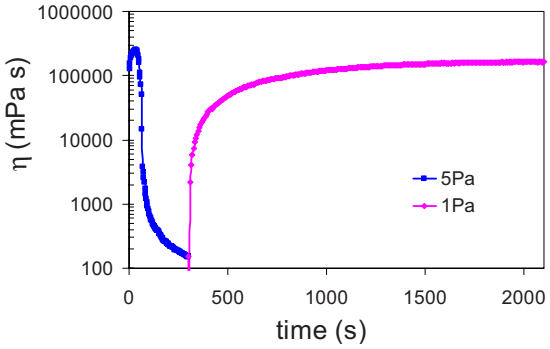

FIG. 7. (Color online) Recovery curve for a 5 mM solution of $[AA9:BB]_n$ in decane at 25 °C.

At concentrations $C \geqslant 5$ mM, that is, in the regime where the polymer chains are entangled, the autocorrelation function of the scattered field becomes bimodal as shown by the example given in Fig. 8. The fast relaxation time τ_c varies as q^{-2}, which is the signature of a collective diffusion process, whereas the slower relaxation time τ_R is independent on q, which indicates a viscoelastic relaxation process [see Fig. 8(b)]. Figures 9(a) and 9(b) show the concentration dependences of $(\tau_c q^2)kT/6\pi\eta_s$ and τ_R, respectively. Also is reported in Fig. 9(c) the q-independent ratio of the amplitudes of the two modes as a function of the concentration obtained

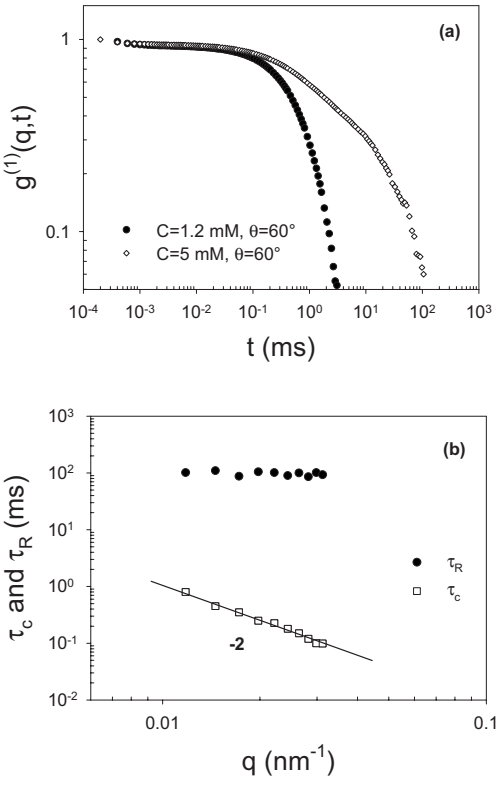

FIG. 8. (a) Log-log representation of $g^{(1)}(q,t)$ for two different $[AA9:BB]_n$ concentrations: $C=1.2$ mM (dilute regime) and $C=5$ mM (semidilute regime). (b) Variation of τ_c and τ_R with q obtained from the fits of $g^{(1)}(q,t)$ in semidilute regime for $C=10$ mM ($C > C^*$).

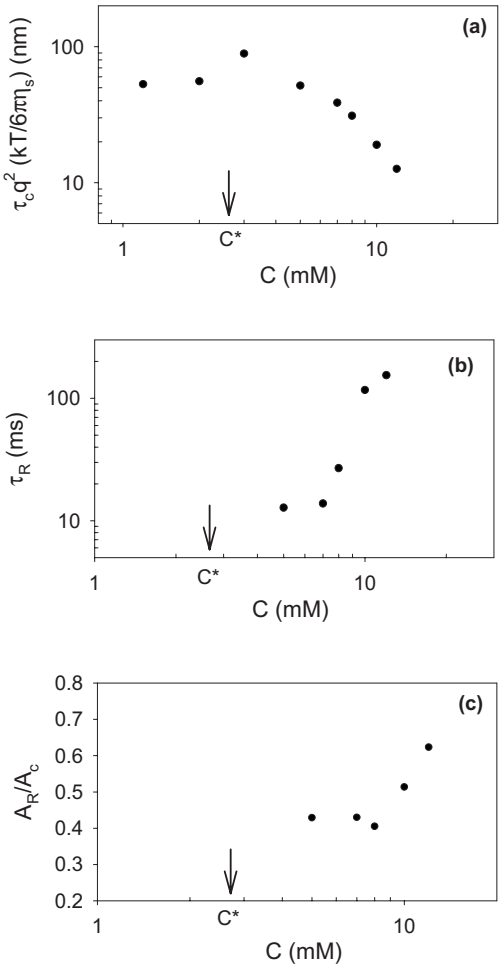

FIG. 9. Variation with $[AA9:BB]_n$ concentration (a) of $(\tau_c q^2)kT/6\pi\eta_s$, (b) of τ_R, and (c) of A_R/A_c.

from the fits of $g^{(1)}(q,t)$. A maximum of $(\tau_c q^2)kT/6\pi\eta_s$ is observed in the vicinity of C^*. Both τ_R and the amplitude ratio increase significantly beyond $C \sim 8$ mM. These features will be discussed in the following.

IV. DISCUSSION

A. Rheological behavior

The abrupt decrease of viscosity by several orders of magnitude at a critical shear rate $\dot{\gamma}_c$, observed in the flow curve of Fig. 5 is similar to those reported for wormlike micelles [50] and for associating polymers [49,51]. Figure 10 gives a representation shear stress versus shear rate of the data of Fig. 5. In this representation, the measured flow curve at controlled mean strain rate $\dot{\gamma}$ exhibits a plateau $\sigma(\dot{\gamma})=\sigma_p$. An explanation of this behavior has been given by Spenley *et al.* [52] who proposed a model based on the reptation mechanism for relaxation of entanglements. Specifically it is found that the stress versus strain-rate curve, $\sigma(\dot{\gamma})$, in homogeneous steady-shear flow is nonmonotonic, which means that there exists a $\dot{\gamma}$ range over which the stress is multivalued as illustrated by Fig. 11. If the applied shear lies in the region of

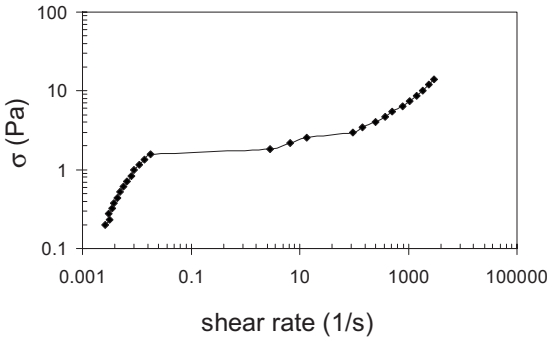

FIG. 10. Shear stress as a function of shear rate for the solution $[AA9:BB]_n$ in decane at $T=25$ °C and $C=5$ mM.

decreasing stress, an initially homogeneous flow becomes mechanically unstable. As a result, the solution evolves up to a stationary state of shearing where bands of highly sheared liquid of low viscosity coexist with a more viscous part supporting a lower rate. In the banded regime, changes in shear rates essentially alter the proportions of the low and high viscosity bands. The stress upturn occurring at high shear rate describes a homogeneous flow of oriented particles and takes into account the solvent contribution. The issue of the selection in the shear banding process and of the value of the stress σ_p shared by the two bands is still a matter of debate. The model initially proposed by Spenley *et al.* postulated that σ_p is at the maximum of the underlying nonmonotonic flow curve occurring at $\dot{\gamma}_c=2.6\ T_R^{-1}$ with $\sigma_p=0.67\times G_0$. The occurrence of shear bands for wormlike micellar systems has been established by experiments [53–56] and good quantitative agreement was found between the prediction of the model with the assumption of top jumping and the experimental data [50,52,57,58]. Some studies have revealed flow curves in which clear departures from top jumping are seen but these studies refer to rather concentrated systems (weight fraction $\approx 5-30$ %). In any case, it has always been found that the stress plateau occurs at a shear rate of the order of T_R^{-1} and has a value of the order of G_0. The results presented in this study are in agreement with both the theoretical predictions and the previous reported experimental data on equilibrium polymers. In particular the stress plateau occurs at a shear rate $\dot{\gamma}=1.2\times 10^{-2}$ s^{-1} as compared to $T_R^{-1} \approx 10^{-2}$ s^{-1}

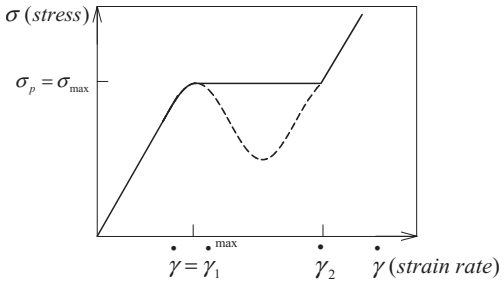

FIG. 11. A nonmonotonic stress vs strain rate curve; the dotted part is unstable. In a banded flow, regions of strain rate $\dot{\gamma}_1$, $\dot{\gamma}_2$ coexist to give a macroscopic mean strain rate $\dot{\gamma}$, which is fixed (under controlled strain rate conditions). The observed flow curve (solid) corresponds to "top jumping:" $\sigma_p=\sigma_{max}$. (From Ref. [52].)

and has a value of 1.39 Pa that is of the same order of magnitude as $G_0 \approx 1$ Pa. There is however some specific features of the system investigated. It is quite remarkable that a pronounced discontinuity in $\dot{\gamma}$, signature of the shear banding instability, is observed for a sample with concentration only twice C^*. For wormlike micellar systems, the instability appears only for samples with $C/C^* \geqslant 20$ [43,44]. This is likely to be due to the formation, inferred from the SANS data, of transient crosslinks between polymeric fibers [39]. Such crosslinks would add their contribution to that of entanglements thus enhancing the plateau modulus and slowing down the reptation process similarly to what is observed for associating polymers [49,59,60]. The second interesting observation concerns the occurrence at high shear rate of a second stress plateau that is possibly associated to a Rouse-like mode. The above results must be compared to those recently obtained on solutions of bis-urea-substituted toluene (EHUT), a bifunctional monomer that assembles reversibly into long polymer chains by multiple hydrogen bonds [61,62]. These systems exhibit a quite complex nonlinear rheological behavior with three different shear-banding regimes appearing successively upon increasing shear rate. The first of these regimes has the features of a mechanical instability characterized by a shear plateau that extends over a much shorter range of shear rates than the one observed in Fig. 10. Such a difference might be linked to the flexibility of the supramolecular chains. The EHUT polymers are quite rigid with a persistence length exceeding 100 nm whereas the persistence length of both the wormlike micelles and the $[\mathrm{AA9:BB}]_n$ polymers is less than 20 nm [38,39,63].

B. Dynamic light scattering

The results of dynamic light scattering must be examined on the light of previous experimental studies and theoretical approaches on solutions of both covalently bonded and equilibrium polymers. In most cases the autocorrelation function of the scattered field is found experimentally to be bimodal as in the present study [64–69]. The origin of the slow mode ranges from cluster [67], to viscoelastic mode [64,65,68], and to well defined chain motions described either by Rouse or reptation models [64,65,69]. In our case, the variation of τ_R presented in Fig. 8(b) supports the presence of a pure q-independent viscoelastic slow mode [64,65].

Several theoretical studies were published on this subject [70–73]. In particular, Semenov derived a full treatment where the relaxation of concentration fluctuations takes into account both deformation of entanglement network and the direct effect of the reptation motion of polymer chains [71]. In this approach, three stages of relaxation of concentration fluctuations are predicted. The first stage is due to cooperative deformation of entanglement network and is characterized by a time:

$$\tau_c = \frac{K}{M_g + K}\left(\frac{kTq^2}{6\pi\eta_s\xi_H}\right)^{-1}, \tag{8}$$

where ξ_H is the hydrodynamic length, η_s the solvent viscosity, M_g the elastic modulus of the entanglement network, and K the bulk modulus. The second stage is a Rouse-type relaxation of the macromolecular tension along the tube with a q-independent relaxation time τ_R. The last stage, associated with the reptation process is characterized by a spectrum of relaxation times with an average time τ_{slow} of the order of the reptation time T_R. Semenov has also calculated the amplitudes of the different relaxational contributions. As a rule, the amplitude of the first cooperative stage A_c is the largest, and the amplitude of the second "Rouse" stage A_R is the smallest. The ratio A_R/A_c is given, in the limit generally encountered $M_g/K \ll 1$ by

$$\frac{A_R}{A_c} \approx \frac{1}{6}\frac{M_g}{K}. \tag{9}$$

For most investigated systems, this ratio is too small to be detected and the autocorrelation function is analyzed in terms of collective diffusion and reptation processes [64,65].

In the present study, the slow relaxation shown in Fig. 8 cannot be attributed to a reptation based mechanism, as the reptation time inferred from the rheological data is much longer than τ_R. For the system at $C=5$ mM, $T_R \sim 100$ s, whereas the relaxation time obtained by DLS is 13 ms. As a matter of fact, evidence of the long relaxation reptational process appears in the recording of the static scattering intensity that exhibits fluctuations at scales of the order of minutes for that concentration. One must then conclude that the slow q-independent mode observed in the DLS experiments is Rouse-like. Its amplitude is larger than for other polymeric systems investigated so far, which indicates a larger elastic modulus M_g. In this respect it must be recalled that small-angle neutron scattering experiments suggested the formation of crosslinks between the polymeric fibers [39]. According to Eq. (9), an increase of crosslink density with concentration would account for the increase of A_R/A_c observed in Fig. 9(c) as M_g increases with the crosslink density, whereas K is independent of this parameter.

The fast mode observed in the DLS data is unambiguously the diffusive mode with characteristic time given by Eq. (8). For linear polymers, the variation of $(\tau_c q^2)kT/6\pi\eta_s$ with concentration reflects that of the hydrodynamic radius in the dilute range and of the apparent hydrodynamic correlation length in the semidilute regime as both K and M_g follow the same scaling law of the concentration. For conventional polymeric systems the latter scales with the concentration according to $\xi_H \sim c^{-0.77}$ [74]. The data of Fig. 9(a) shows an enhanced decrease at high concentration, likely due to the increase of $M_g/(K+M_g)$ resulting from an increase of the crosslinks density [cf. Eq. (8)]. It must also be noted that the linear viscoelasticity results shown in Fig. 2(b) indicate the presence of Rouse-like mode with a characteristic time smaller than 20 ms, which is in agreement with the DLS result that yields a value $\tau_R \sim 15$ ms.

V. CONCLUSION

The main result obtained in the above rheological study is the observation of a shear banding type instability in the flow experiments. This instability that has been predicted theoretically for both regular covalently bonded polymers and equi-

librium polymers has been mainly observed for wormlike micellar systems. The stress plateau or equivalently the discontinuity of viscosity occurs at a critical shear rate $\dot{\gamma}_c$ of the order of magnitude of the inverse relaxation time of the stress in the linear regime and has a value close to that of the shear plateau modulus in agreement with the theoretical predictions.

Still, the experiments do not allow us to draw conclusions concerning the breaking time of the polymers as the analysis of the main relaxation spectrum is not feasible, this spectrum being located at frequencies much lower than the experimental window.

The very low concentration at which the shear instability occurs and the very long terminal time of the stress relaxation suggest that temporary interfibers junctions form as soon as the polymeric fibers overlap each other. An interesting feature concerns the presence in the high $\dot{\gamma}$ range, before the stress upturn, of a second regime of still inhomogeneous flow where the rheology of the viscous bands would be controlled by Rouse relaxation. In this respect, it must be pointed out that the theoretical models developed to describe the linear viscoelasticity of associating polymers, based on the sticky reptation mechanism, predict a bimodal stress relaxation with a high frequency mode controlled by the life time of the temporary interchain junctions[59].

The DLS results show also the presence of a Rouse mode of much larger amplitude than in conventional polymer systems. The analysis of this mode allows concluding that the increase of the elastic modulus of the solution with concentration is enhanced with respect to that of entangled solutions of linear polymers. This explains also why the decrease of the apparent hydrodynamic correlation length in the semidilute regime is faster than the scaling behavior of linear polymer. It remains to see whether the original features of the dynamical behavior reported in this study are common to all supramolecular polymer systems.

ACKNOWLEDGMENTS

The authors gratefully acknowledge J. Selb for his help during the rheological measurements.

[1] *Supramolecular Polymers*, 2nd ed., edited by A. Ciferri (Taylor & Francis, Boca Raton, FL, 2005).
[2] L. Brunsveld, B. J. B. Folmer, E. W. Meijer, and R. P. Sijbesma, Chem. Rev. (Washington, D.C.) **101**, 4071 (2001).
[3] J. M. Lehn, Polym. Int. **51**, 825 (2002).
[4] J. S. Moore, Curr. Opin. Colloid Interface Sci. **4**, 108 (1999).
[5] C. M. Paleos and D. Tsiourvas, Adv. Mater. (Weinheim, Ger.) **9**, 695 (1997).
[6] D. C. Sherrington and K. A. Taskinen, Chem. Soc. Rev. **30**, 83 (2001).
[7] C. Schmuck and W. Wienand, Angew. Chem., Int. Ed. **40**, 4363 (2001).
[8] Proc. Natl. Acad. Sci. U.S.A. (special edition on Self Assembly Processes) **99**, 8 (2002).
[9] C. Fouquey, J. M. Lehn, and A. M. Levelut, Adv. Mater. (Weinheim, Ger.) **2**, 254 (1990).
[10] L. J. Prins, D. N. Reinhoudt, and P. Timmerman, Angew. Chem. **113**, 2446 (2001).
[11] K. Hirschberg, J. Brunsveld, A. Ramzi, J. A. J. Vekemans, R. P. Sijbesma, and E. W. Meijer, Nature (London) **38**, 2870 (2000).
[12] O. Ikkala and G. ten Brinke, Science **295**, 2407 (2002).
[13] M. Kotera, J. M. Lehn, and J. P. Vigneron, J. Chem. Soc., Chem. Commun. **1994**, 197 (1994).
[14] M. Kotera, J. M. Lehn, and J. P. Vigneron, Tetrahedron **51**, 1953 (1995).
[15] J. M. Lehn, M. Mascal, A. DeCian, and J. Fischer, J. Chem. Soc., Chem. Commun. **1990**, 479 (1990).
[16] J. M. Lehn, M. Mascal, A. DeCian, and J. Fischer, J. Chem. Soc., Perkin Trans. 1 **1992**, 461 (1992).
[17] V. Berl, M. Schmutz, M. J. Krische, R. G. Khoury, and J. M. Lehn, Chem.-Eur. J. **8**, 1227 (2002).
[18] M. Ikeda, T. Nobori, M. Schmutz, and J. M. Lehn, Chem.-Eur. J. **11**, 662 (2005).
[19] R. P. Sijbesma, F. H. Beijer, L. Brunsveld, B. J. B. Folmer, J. H. K. Hirschberg, R. F. M. Lange, J. K. L. Lowe, and E. W. Meijer, Science **278**, 1601 (1997).
[20] B. J. B. Folmer, E. Cavini, R. P. Sijbesma, and E. W. Meijer, Chem. Commun. (Cambridge) **1998**, 1847 (1998).
[21] C. P. Lillya, R. J. Baker, S. Hütte, H. H. Winter, Y. G. Lin, J. Shi, C. Dickinson, and J. C. W. Chien, Macromolecules **25**, 2076 (1992).
[22] C. M. Lee, C. P. Jariwala, and A. C. Griffin, Polymer **35**, 4550 (1994).
[23] P. Bladon and A. C. Griffin, Macromolecules **26**, 6604 (1993).
[24] C. Alexander, C. P. Jariwala, C. M. Lee, and A. C. Griffin, Macromol. Chem., Macromol. Symp. **77**, 283 (1994).
[25] C. B. St. Pourcain and A. C. Griffin, Macromolecules **28**, 4116 (1995).
[26] I. S. Choi, X. Li, E. E. Simanek, R. Akaba, and G. M. Whitesides, Chem. Mater. **11**, 684 (1999).
[27] S. Abed, S. Boileau, L. Bouteiller, and N. Lacoudre, Polym. Bull. (Berlin) **39**, 317 (1997).
[28] C. He, C. M. Lee, A. C. Griffin, L. Bouteiller, N. Lacoudre, S. Boileau, C. Fouquet, and J. M. Lehn, Mol. Cryst. Liq. Cryst. Sci. Technol., Sect. A **332**, 251 (1999).
[29] F. Lortie, S. Boileau, L. Bouteiller, C. Chassenieux, B. Demé, G. Ducouret, M. Jalabert, F. Laupretre, and P. Terech, Langmuir **18**, 7218 (2002).
[30] T. Kato, M. Fujumasa, and J. M. J. Fréchet, Chem. Mater. **7**, 368 (1995).
[31] H. Kihara and J. M. J. Fréchet, Liq. Cryst. **24**, 413 (1998).
[32] H. Kihara, T. Kato, T. Uryu, and J. M. J. Fréchet, Chem. Mater. **8**, 961 (1996).
[33] T. Kato, H. Kihara, U. Kumar, T. Uryu, and J. M. J. Fréchet, Angew. Chem., Int. Ed. Engl. **33**, 1644 (1994).
[34] T. Kato, O. Ihata, S. Ujiie, M. Tokita, and J. Watanabe, Macromolecules **31**, 3551 (1998).

[35] T. Kato, Y. Kubota, M. Nakano, and T. Uryu, Chem. Lett. **1995**, 1127 (1995).
[36] R. K. Castellano, D. M. Rudkevich, and J. Rebek, Jr., Proc. Natl. Acad. Sci. U.S.A. **94**, 7132 (1997).
[37] C. T. Seto and G. M. Whitesides, J. Am. Chem. Soc. **115**, 905 (1993).
[38] E. Kolomiets, E. Buhler, S. J. Candau, and J. M. Lehn, Macromolecules **39**, 1173 (2006).
[39] E. Buhler, S. J. Candau, J. Schmidt, Y. Talmon, E. Kolomiets, and J. M. Lehn, J. Polym. Sci., Part B: Polym. Phys. **45**, 103 (2007).
[40] R. M. Versteegen, D. J. M. van Beek, R. P. Sijbesma, D. Vlassopoulos, G. Fytas, and E. W. Meijer, J. Am. Chem. Soc. **127**, 13862 (2005).
[41] H. Kautz, D. J. M. van Beek, R. P. Sijbesma, and E. W. Meijer, Macromolecules **39**, 4265 (2006).
[42] D. J. M. van Beek, M. A. J. Gillissen, B. A. C. van As, A. R. A. Palmans, and R. P. Sijbesma, Macromolecules **40**, 6340 (2007).
[43] C. Grand, J. Arrault, and M. E. Cates, J. Phys. II **7**, 1071 (1997).
[44] J. F. Berret, D. C. Roux, and G. Porte, J. Phys. II **4**, 1261 (1994).
[45] K. S. Schmitz, *An Introduction to Dynamic Light Scattering by Macromolecules* (Academic Press, London, 1990).
[46] D. E. Koppel, J. Chem. Phys. **57**, 4814 (1972).
[47] S. W. Provencher, Makromol. Chem. **82**, 632 (1985).
[48] K. te Nijenhuis, Adv. Polym. Sci. **130**, 1 (1997).
[49] P. Kujawa, A. Audibert-Hayet, J. Selb, and F. Candau, J. Polym. Sci., Part B: Polym. Phys. **42**, 1640 (2004).
[50] A. Khatory, F. Lequeux, F. Kern, and S. J. Candau, Langmuir **9**, 1456 (1993).
[51] T. Aubry and M. Moan, J. Rheol. **40**, 441 (1996).
[52] N. A. Spenley, M. E. Cates, and T. C. B. McLeish, Phys. Rev. Lett. **71**, 939 (1993).
[53] R. Makhloufi, J. P. Decruppe, A. Ait-Ali, and R. Cressely, Europhys. Lett. **32**, 253 (1995).
[54] J. P. Decruppe, R. Cressely, R. Makhloufi, and E. Cappelaere, Colloid Polym. Sci. **273**, 346 (1995).
[55] R. W. Mair and P. T. Callaghan, Europhys. Lett. **65**, 241 (1996).
[56] P. T. Callaghan, M. E. Cates, C. J. Rofe, and J. B. A. F. Smeulders, J. Phys. II **6**, 375 (1996).
[57] H. Rehage and H. Hoffmann, Mol. Phys. **74**, 933 (1991).
[58] H. Rehage and H. Hoffmann, J. Phys. Chem. **92**, 4712 (1988).
[59] L. Leibler, M. Rubinstein, and R. H. Colby, Macromolecules **24**, 4701 (1991).
[60] M. Rubinstein and A. N. Semenov, Macromolecules **34**, 1058 (2001).
[61] J. van der Gucht, M. Lemmers, W. Knoben, N. A. M. Besseling, and M. P. Lettinga, Phys. Rev. Lett. **97**, 108301 (2006).
[62] J. van der Gucht, N. A. M. Besseling, W. Knoben, L. Bouteiller, and M. A. Cohen Stuart, Phys. Rev. E **67**, 051106 (2003).
[63] G. Porte, J. Appell, and Y. Poggi, J. Phys. Chem. **84**, 3105 (1980).
[64] M. Adam and M. Delsanti, Macromolecules **18**, 1760 (1985).
[65] E. Buhler, J. P. Munch, and S. J. Candau, J. Phys. II **5**, 765 (1995).
[66] M. Takenaka, S. Nishitsuji, and H. Hasegawa, J. Chem. Phys. **126**, 064903 (2007).
[67] G. Yuan, X. Wang, C. C. Han, and C. Wu, Macromolecules **39**, 6207 (2006).
[68] T. Jian, D. Vlassopoulos, G. Fytas, T. Pakula, and W. Brown, Colloid Polym. Sci. **274**, 1033 (1996).
[69] N. Boudenne, S. H. Anastasiadis, G. Fytas, M. Xenidou, N. Hadjichristidis, A. N. Semenov, and G. Fleischer, Phys. Rev. Lett. **77**, 506 (1996).
[70] F. Brochard and P. G. de Gennes, Macromolecules **10**, 121 (1985).
[71] A. N. Semenov, Physica A **166**, 263 (1990).
[72] M. Doi and A. Onuki, J. Phys. II **2**, 1631 (1992).
[73] C. H. Wang, Macromolecules **25**, 1524 (1992).
[74] P. G. de Gennes, *Scaling Concepts in Polymer Physics* (Cornell University Press, Ithaca, 1979).